Published by

British Journal of Contemporary Research

BEXFORD PUBLISHING

Comparative Major-Oxide and Trace-Element Characterization of Activated Carbon, Sawdust-Derived Carbon, and Rice-Husk-Derived Carbon for Preliminary Water-Treatment Assessment

Original Research Article | Volume 1 | Issue 4 | 2026 | Article Number: 037

Accepted: 31 August 2026 | Published: 10 September 2026 | ISSN: 2979-8582 (Online)

Crossref : **https://doi.org/10.67693/BJCR-TLRIT8XP**

Abiodun B LANIYAN[1], Olusola O OYEWOLE[2], Opeyemi O OGUNYINKA[3], Olawale D Williams[4], Olaide I Afolabi[5]

[1]Department of Science Laboratory Technology: Water Resources and Environmental Engineering, D.S Adegbenro ICT Polytechnic, Itori-Ewekoro, Nigeria,

[2]Society for Family Health, Nigeria, Demand Generation, Communications, Social and Behavior Change, Nigeria,

[3]Department of Science Laboratory Technology: Environmental Chemistry, D.S Adegbenro ICT Polytechnic, Itori-Ewekoro, Nigeria,

[4]Department of Science Laboratory Technology: Biochemistry, D.S Adegbenro ICT Polytechnic, Itori-Ewekoro, Nigeria,

[5]Department of Science Laboratory Technology: Chemistry, D.S Adegbenro ICT Polytechnic, Itori-Ewekoro, Nigeria

ABL 0009-0002-2046-1720 , **OOO** 0000-0002-8347-8506 , **OOO** 0009-0002-0736-3368

Correspondence: Abiodun B LANIYAN, abiodunlaniyan@gmail.com

Abstract

Activated carbon (AC), sawdust-derived carbon (SDC), and rice-husk-derived carbon (RHC) were comparatively characterized to assess major-oxide and trace-element differences relevant to preliminary water-treatment adsorbent screening. Sawdust and rice husk were washed, oven-dried at 80 °C for 12 h, and thermally treated at 550 °C for 30 min; the activated carbon was commercially obtained. X-ray fluorescence analysis was performed on pressed pellets using a Philips PW-1800 spectrometer, with duplicate analytical measurements for each material. SiO_2 was the dominant reported oxide, with concentrations of 68.42 wt.% in AC, 54.76 wt.% in SDC, and 73.18 wt.% in RHC. The oxide profiles indicated comparatively Si-Al-associated, Ca-Mg-Fe-associated, and Si-K-P-associated signatures for AC, SDC, and RHC, respectively. SDC recorded the highest concentrations of 10 of the 13 measured trace elements, whereas RHC recorded the highest Ba, Sr, and Rb concentrations. Reported SiO_2 relative standard deviations ranged from 1.6 to 2.4%, indicating low analytical dispersion in the duplicate measurements. The results demonstrate clear compositional differentiation among the three materials and support composition-based preliminary screening, but they do not establish adsorption performance, contaminant-removal efficiency, or trace-element leaching.

Keywords: Activated Carbon, Sawdust-Derived Carbon, Rice-Husk-Derived Carbon, X-Ray Fluorescence, Major Oxides, Trace Elements, Water Treatment

1. INTRODUCTION

Adsorption is an established physicochemical process for the removal of contaminants from water and wastewater, and activated carbon remains one of the most widely used carbonaceous adsorbents. Its effectiveness is commonly associated with developed porosity, relatively high specific surface area, and chemically active surface sites capable of interacting with a range of dissolved contaminants (Ahmad et al., 2014; Mohan et al., 2014; Tan et al., 2015). Increasing attention has also been directed toward biomass-derived carbonaceous materials because agricultural and lignocellulosic residues can provide comparatively accessible precursors for adsorbent production while supporting waste valorization and more circular approaches to resource use (Liu et al., 2015; Marzeddu et al., 2022).

Sawdust and rice husk are representative lignocellulosic residues that can be converted into carbonaceous materials through thermochemical processing. However, carbonaceous materials derived from different precursors should not be assumed to possess equivalent physicochemical or inorganic characteristics. Their interactions with aqueous contaminants may involve several processes, including pore filling, electrostatic interactions, ion exchange, surface complexation, and reactions involving inorganic constituents, with the relative importance of each mechanism depending on adsorbent characteristics, contaminant properties, and solution chemistry (Ahmad et al., 2014; Mohan et al., 2014; Tan et al., 2015). Consequently, comparative assessment of carbonaceous adsorbents requires consideration not only of the carbon matrix but also of the associated inorganic composition.

The physicochemical characteristics of biomass-derived carbonaceous materials are strongly influenced by both feedstock composition and processing history. Factors such as biomass type, precursor mineral content, carbonization or pyrolysis temperature, residence time, reaction atmosphere, activation procedure, washing, and post-treatment can modify porosity, surface chemistry, ash content, and the retention or transformation of inorganic constituents (Liu et al., 2015; Karam et al., 2022; Marzeddu et al., 2022). Thermal conversion removes part of the volatile and organic fraction of biomass and can thereby increase the relative contribution of non-volatile inorganic constituents in the resulting solid. At the same time, individual elements may undergo transformation, redistribution, or loss depending on their chemical form and processing conditions. Consequently, the inorganic composition of a carbonaceous product can differ substantially from that of its original precursor.

This consideration is particularly relevant to rice husk, which is well recognized for its substantial biogenic silica content. Previous studies have demonstrated that rice-husk-derived carbonaceous materials can retain considerable quantities of silica following thermal or hydrothermal conversion (Hossain et al., 2020; Morales et al., 2021; Karam et al., 2022). Russo et al. (2023) further demonstrated that mineral constituents form an important component of the structure and physicochemical behaviour of rice-husk-derived adsorbent materials. Nevertheless, absolute silica concentrations can vary among studies because of differences in feedstock characteristics, thermal conditions, washing or pretreatment, residual carbon content, and the analytical basis used to express composition (Karam et al., 2022; Taiye et al., 2024). Feedstock identity and processing history can therefore generate distinct inorganic compositional signatures in carbonaceous materials, which may influence their behaviour at the solid–water interface.

Major-oxide characterization provides a useful means of describing the inorganic fraction of carbonaceous materials. Frequently reported oxide-equivalent constituents include SiO_2, Al_2O_3, Fe_2O_3, TiO_2, CaO, MgO,

K_2O, P_2O_5, MnO, and Na_2O. Differences in their relative abundance can help distinguish carbonaceous materials derived from different feedstocks or processing histories and can identify compositional features potentially relevant to environmental applications (Marzeddu et al., 2022; Russo et al., 2023). Silica is of particular interest in rice-husk-derived materials because rice plants accumulate substantial quantities of biogenic silica, and thermal conversion can therefore yield materials with pronounced silica-associated inorganic characteristics (Hossain et al., 2020; Morales et al., 2021; Karam et al., 2022; Taiye et al., 2024).

However, high bulk SiO_2 concentration should not, by itself, be interpreted as evidence of enhanced adsorption performance because contaminant retention also depends on properties such as surface accessibility, pore structure, surface functional groups, and solution conditions. Similarly, Ca- and Mg-bearing constituents may contribute to ion exchange, surface complexation, or precipitation-related interactions under appropriate aqueous conditions, while Fe- and Al-bearing components can provide chemically reactive sites for interaction with selected dissolved species. The extent to which such processes occur depends on the chemical form of the inorganic constituents, their surface accessibility, contaminant speciation, pH, ionic strength, and the presence of competing ions (Ahmad et al., 2014; Mohan et al., 2014; Liu et al., 2015). Importantly, bulk oxide-equivalent concentrations do not establish the presence, crystallinity, mineralogical identity, or surface accessibility of specific mineral phases.

In addition to major-oxide composition, the intrinsic trace-element inventory of carbonaceous materials is relevant to their environmental characterization. Biomass-derived and activated carbonaceous materials may contain trace quantities of elements such as Ba, Cu, Cr, Ni, Zn, Co, Sr, Pb, Cd, and others arising from the precursor material, associated inorganic matter, environmental exposure, or processing history (Marzeddu et al., 2022; Dong et al., 2025). Trace-element characterization serves two complementary purposes. First, elemental profiles can assist in distinguishing carbonaceous materials with different precursor or production histories. Second, characterization of the adsorbent itself is important when considering environmental use because material selection should account not only for potentially beneficial contaminant-retention characteristics but also for the adsorbent's intrinsic chemical composition. Recent assessments of biochar applications have increasingly emphasized the need to consider potential unintended chemical effects alongside intended environmental benefits (Dong et al., 2025).

Total solid-phase concentration, however, should not be equated with environmental mobility or exposure. A concentration expressed as mg kg^{-1} of solid material cannot be compared directly with an aqueous water-quality criterion expressed in mg L^{-1} or µg L^{-1}. Moreover, only a fraction of an element present in a solid may become soluble or mobile under a particular set of environmental conditions. Assessment of leaching, mobility, bioavailability, or aqueous exposure therefore requires appropriate extraction, leaching, or water-contact measurements.

Previous studies have demonstrated the potential relevance of activated carbon and biomass-derived carbonaceous materials for water-treatment applications, including materials derived from sawdust and rice husk. In particular, Adekunle et al. (2020) comparatively characterized activated charcoal, sawdust charcoal, and rice-husk charcoal in the context of water treatment. The existence of such previous work means that the present investigation should not be framed as the first comparison of these three broad material classes. Rather, the rationale for the present study lies in the systematic integration of multiple aspects of inorganic chemical characterization within a common comparative framework.

Although individual studies have examined major mineral constituents, surface characteristics, or adsorption-related properties of different carbonaceous materials, there remains value in jointly evaluating major-oxide distributions, selected oxide-equivalent groupings, trace-element inventories, environmentally relevant trace elements, inter-material concentration contrasts, and available analytical-precision

information when comparing candidate carbonaceous adsorbents. Accordingly, the present study examines ten reported major oxides and thirteen trace elements in activated carbon, sawdust-derived carbon, and rice-husk-derived carbon. Particular attention is given to Cu, Cr, Ni, Zn, Pb, and Cd because of their environmental relevance. Selected oxide combinations are used as descriptive indicators of broader inorganic compositional patterns, while maximum-to-minimum concentration ratios are used to quantify the magnitude of inter-material compositional contrasts. Available analytical precision information for SiO_2 is additionally considered to provide quality-control context for the dominant reported oxide.

The aim of this study was to comparatively characterize the major-oxide and trace-element compositions of activated carbon, sawdust-derived carbon, and rice-husk-derived carbon and assess the implications of their compositional differences for preliminary selection as water-treatment adsorbent materials. Specifically, the study sought to determine and compare the major-oxide profiles of the three materials; evaluate selected oxide groupings as descriptive indicators of broader inorganic compositional differences; characterize and compare their trace-element profiles; examine environmentally relevant trace elements, particularly Cu, Cr, Ni, Zn, Pb, and Cd; quantify inter-material compositional contrasts using descriptive maximum-to-minimum concentration ratios; evaluate the available analytical precision information for SiO_2 using relative standard deviation; and integrate the major-oxide and trace-element characteristics to provide a preliminary chemical basis for comparing the three carbonaceous materials as candidate adsorbent materials.

Accordingly, the scope of the study is restricted to comparative chemical characterization and preliminary material screening. It does not directly determine adsorption capacity, contaminant-removal efficiency, adsorption kinetics, adsorption isotherms, regeneration performance, trace-element leaching, or environmental risk. Conclusions concerning these properties therefore fall outside the analytical scope of the present dataset.

2. MATERIALS AND METHODS

2.1 Materials and Equipment

Three carbonaceous materials were investigated: activated carbon (AC), sawdust-derived carbon (SDC), and rice-husk-derived carbon (RHC). The activated carbon was purchased in Ijebu Ode, Nigeria. Sawdust was collected from a sawmill in Abeokuta, Nigeria, while rice husk was collected as a biomass precursor.

The principal materials and equipment used included sawdust (nominal particle size, 1 mm), rice husk (1 mm), activated carbon (2 mm), 1- and 2-mm sieves, a laboratory oven, a Vecstar furnace, an electric crusher, a Herzog Gyro-mill (Simatic C7-621), Herzog pelletizing equipment, and a Philips PW-1800 X-ray fluorescence (XRF) spectrometer.

2.2 Preparation of Carbonaceous Materials

The activated carbon was sieved to obtain a nominal particle size of 2 mm. Sawdust collected from the sawmill in Abeokuta was sieved to obtain a nominal particle size of 1 mm, while the rice husk was ground and sieved to obtain a nominal particle size of 1 mm.

The sawdust and rice husk were washed and subsequently oven-dried at 80 °C for 12 h. After drying, each biomass material was separately subjected to thermal treatment in a Vecstar furnace at 550 °C for 30 min. Following thermal treatment, the resulting carbonaceous materials were allowed to cool and were subsequently air-dried. The products obtained from sawdust and rice husk were designated sawdust-derived carbon (SDC) and rice-husk-derived carbon (RHC), respectively. The commercially obtained activated carbon was designated AC.

The available experimental record does not specify the furnace atmosphere or heating rate; these parameters were therefore not assumed in describing the preparation procedure.

2.3 X-Ray Fluorescence Analysis

The major-oxide and trace-element compositions of AC, SDC, and RHC were determined using a Philips PW-1800 X-ray fluorescence spectrometer.

Before XRF analysis, each carbonaceous material was crushed using an electric crusher and pulverized for 60 s using a Herzog Gyro-mill (Simatic C7-621). The milling equipment was cleaned after preparation of each sample to minimize the possibility of cross-contamination.

For pellet preparation, 20 g of pulverized sample was mixed with 0.4 g of stearic acid and ground for 60 s. Stearic acid was used during pellet preparation as a binding material. The prepared material was subsequently transferred into an aluminium cup and compacted using Herzog pelletizing equipment at a pressure of 200 kN for 60 s.

The prepared pellets were placed in the sample holder of the Philips PW-1800 XRF spectrometer for analysis. The same preparation and analytical procedure was applied to AC, SDC, and RHC. Duplicate analytical measurements (n = 2) were obtained for each material.

The XRF results were reported as oxide-equivalent concentrations in weight percent (wt.%) for the major components and as parts per million (ppm) for the reported trace elements. For the solid samples, ppm values were expressed in the Results as mg kg^{-1} on a mass basis (1 ppm = 1 mg kg^{-1}). The available analytical record did not explicitly state whether the oxide percentages were reported on a whole-sample, ash, or normalized inorganic basis; the reported values were therefore used without re-normalization.

The major oxides evaluated were SiO_2, Al_2O_3, Fe_2O_3, TiO_2, CaO, P_2O_5, K_2O, MnO, MgO, and Na_2O. The trace elements evaluated were Ba, Cu, Cr, Ni, Zn, Co, Sr, Pb, Sc, Cd, Nb, Rb, and Zr.

2.4 Data Processing and Analytical Precision

The XRF data were used to compare the inorganic compositions of AC, SDC, and RHC. Major-oxide concentrations were expressed in wt.%, whereas trace-element concentrations were expressed as mg kg^{-1}. The Other/undetermined fraction was retained as reported because the available analytical record did not state whether this fraction was measured independently or calculated by difference. No chemical identity was assigned to this residual fraction.

The duplicate analytical measurements were examined to assess the consistency of the determinations. Where replicate values were available, relative standard deviation (RSD) was calculated as:

$$\text{RSD}\ (\%) = (s / \bar{x}) \times 100$$

where s is the standard deviation of the replicate measurements and $\bar{x}$ is their arithmetic mean.

Because the documented procedure involved duplicate analytical measurements (n = 2) per material rather than independent replicate material batches, the resulting variability was interpreted as analytical repeatability and was not used as a basis for inferential statistical testing.

The compositional data were therefore compared descriptively among AC, SDC, and RHC. Differences were reported as observed differences in measured concentrations and were not described as statistically significant.

2.5 Quality Assurance and Analytical Limitations

The available laboratory records document the XRF sample-preparation procedure, analytical instrument,

and use of duplicate measurements for each material. However, the records available for the present study do not provide sufficient information concerning certified reference materials, calibration-verification procedures, analytical blanks, spike recoveries, method-specific limits of detection, or limits of quantification. Accordingly, these procedures have not been assumed or retrospectively introduced. Interpretation of the lowest reported trace-element concentrations, particularly Cd and Nb, is therefore constrained by the absence of documented method-specific detection and quantification limits.

The analytical results were interpreted within the limitations of the documented procedures. XRF measurements were treated as bulk compositional measurements of the analysed materials. The reported trace-element concentrations represent solid-phase concentrations and were not interpreted as measurements of leachability, bioavailability, or environmental exposure.

Likewise, oxide-equivalent concentrations were used as compositional descriptors and were not considered, by themselves, evidence for the presence or identity of particular mineralogical phases. Mineralogical identification would require complementary techniques specifically designed for phase identification.

2.6 Data Interpretation

The major-oxide and trace-element results were used to establish comparative chemical profiles for AC, SDC, and RHC. Differences in oxide composition were evaluated to identify the dominant compositional characteristics of each material, while trace-element concentrations were examined to provide an additional description of their inorganic inventories.

The chemical characterization was used to support preliminary comparison of the three carbonaceous materials for potential water-treatment applications. However, the characterization data alone were not used to claim differences in adsorption capacity, contaminant-removal efficiency, adsorption kinetics, regeneration performance, mineral phase identity, or leaching behaviour.

This approach ensured that interpretation of the analytical results remained within the scope supported by the measurements actually performed.

3. RESULTS AND DISCUSSION

3.1 Major-Oxide Composition of the Carbonaceous Materials

The three carbonaceous materials exhibited distinct major-oxide profiles (Table 1; Figure 1). SiO_2 was the dominant reported oxide in all three materials, with concentrations of 68.42 wt.% in activated carbon (AC), 54.76 wt.% in sawdust-derived carbon (SDC), and 73.18 wt.% in rice-husk-derived carbon (RHC). The concentrations therefore followed the order RHC > AC > SDC and ranged from 54.76 to 73.18 wt.%. The difference between RHC and SDC was 18.42 percentage points, while the SiO_2 proportion in RHC was approximately 1.34 times that of SDC. Because only duplicate analytical measurements were available and no independent replicate material batches or inferential statistical tests were used, the observed differences are treated as descriptive compositional contrasts rather than statistically significant differences.

Table 1. Major-oxide composition of activated carbon, sawdust-derived carbon, and rice-husk-derived carbon.

Major oxide	AC (wt.%)	SDC (wt.%)	RHC (wt.%)
SiO_2	68.42	54.76	73.18
Al_2O_3	4.21	3.18	2.74

Major oxide	AC (wt.%)	SDC (wt.%)	RHC (wt.%)
Fe_2O_3	1.36	1.92	0.88
TiO_2	0.18	0.27	0.31
CaO	3.84	5.63	4.92
P_2O_5	0.72	1.18	1.43
K_2O	4.26	6.47	7.84
MnO	0.09	0.16	0.24
MgO	1.74	2.86	1.31
Na_2O	0.31	0.48	0.36
Other/undetermined	14.87	23.09	6.79
Total	**100.00**	**100.00**	**100.00**

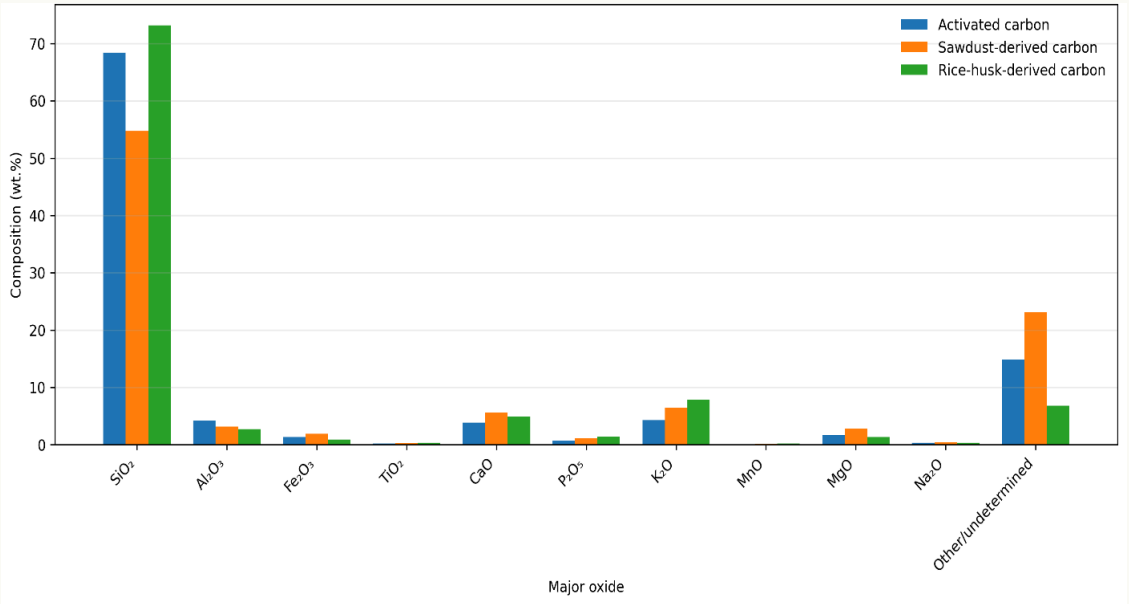

Figure 1. Major-oxide composition of activated carbon, sawdust-derived carbon, and rice-husk-derived carbon.

The comparatively high SiO_2 concentration in RHC indicates a pronounced silica-rich inorganic signature. This pattern is consistent with the established composition of rice husk and rice-husk-derived carbonaceous materials. Hossain et al. (2020) showed that conversion of rice husk to biochar retains important inorganic components, while Morales et al. (2021) reported substantial silica retention following rice-husk pyrolysis. Karam et al. (2022) likewise identified silica as a characteristic component of rice-husk biochar, and Russo et al. (2023) demonstrated that silica and other mineral constituents remain structurally integrated within rice-husk-derived adsorbents. The 73.18 wt.% SiO_2 observed in RHC is therefore consistent with the silica-rich nature reported for thermally converted rice husks. Nevertheless, absolute SiO_2 concentrations should not be expected to be identical among studies because they can vary with feedstock origin, thermal-conversion conditions, pretreatment or washing, residual carbon content, and the analytical basis used to express oxide composition (Hossain et al., 2020; Karam et al., 2022; Taiye et al., 2024).

Differences among the lower-concentration oxides further differentiated the materials. AC contained the highest Al_2O_3 concentration (4.21 wt.%). SDC recorded the highest Fe_2O_3 (1.92 wt.%), CaO (5.63 wt.%), MgO (2.86 wt.%), and Na_2O (0.48 wt.%), whereas RHC had the highest TiO_2 (0.31 wt.%), P_2O_5 (1.43 wt.%), K_2O (7.84 wt.%), and MnO (0.24 wt.%). Because SiO_2 dominates the overall oxide profiles in Figure 1, the secondary differences are more clearly illustrated in Figure 2.

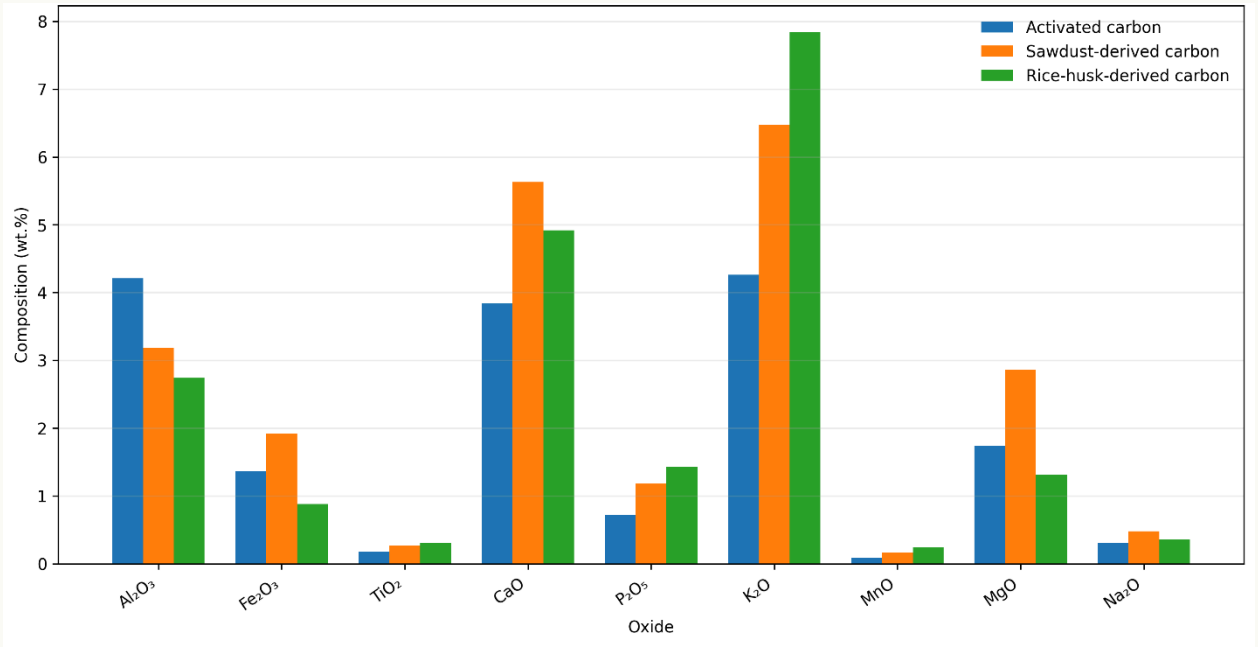

Figure 2. Comparative distribution of secondary major oxides in activated carbon, sawdust-derived carbon, and rice-husk-derived carbon, excluding SiO_2 and the Other/undetermined fraction.

In addition to its silica-rich composition, RHC exhibited comparatively elevated K_2O and P_2O_5 concentrations of 7.84 and 1.43 wt.%, respectively. Relative to AC, these values were approximately 84.0% and 98.6% higher, respectively. The simultaneous enrichment of SiO_2, K_2O, and P_2O_5 therefore gives RHC a distinctive Si–K–P-associated compositional signature. Rice-husk-derived materials have similarly been reported to retain silica together with varying amounts of K-, P-, Ca-, Mg-, and other inorganic constituents (Karam et al., 2022; Russo et al., 2023; Taiye et al., 2024). These proportions can vary with biomass composition and thermal processing. The elevated K_2O and P_2O_5 concentrations observed here should therefore be interpreted as compositional characteristics rather than as evidence of enhanced adsorption performance.

SDC showed a contrasting oxide pattern, with the highest CaO, MgO, and Fe_2O_3 concentrations among the three materials. Relative to AC, SDC contained approximately 46.6% more CaO, 64.4% more MgO, and 41.2% more Fe_2O_3. The combined CaO + MgO + Fe_2O_3 fraction was 10.41 wt.% in SDC, compared with 6.94 wt.% in AC and 7.11 wt.% in RHC. SDC can therefore be described as exhibiting a comparatively Ca–Mg–Fe-enriched inorganic profile. Such variability is compatible with the established influence of feedstock composition and processing history on carbonaceous sorbents. Marzeddu et al. (2022), for example, reported substantial physicochemical differences among carbon-based sorbents derived from different starting materials and preparation routes. The Ca–Mg–Fe enrichment observed in the present SDC should consequently be interpreted as a characteristic of the investigated material rather than as a universal feature of sawdust-derived carbon or as evidence of superior adsorption performance.

AC was distinguished particularly by its Al_2O_3 concentration of 4.21 wt.%, compared with 3.18 wt.% in SDC and 2.74 wt.% in RHC. These differences correspond to approximately 32.4% and 53.6% higher Al_2O_3 concentrations in AC than in SDC and RHC, respectively. Together with its comparatively high SiO_2

concentration, the AC sample can therefore be characterized by a Si–Al-associated inorganic signature. Activated carbons are chemically heterogeneous materials, and their residual inorganic composition can depend on precursor type, activation process, thermal history, washing, and ash removal. Comparative characterization of carbon-based sorbents likewise indicates that substantial differences can occur among activated and biomass-derived carbons because of precursor and processing conditions (Marzeddu et al., 2022). The AC profile observed here should therefore be regarded as specific to the investigated material.

The Other/undetermined fraction represented 14.87 wt.% of AC, 23.09 wt.% of SDC, and 6.79 wt.% of RHC. Consequently, the ten individually reported oxides accounted for 85.13%, 76.91%, and 93.21% of AC, SDC, and RHC, respectively. Inclusion of the residual fraction brought each compositional profile to 100.00 wt.%. If this fraction was obtained by difference rather than independently quantified, it should be treated only as an unaccounted or residual fraction. In the absence of additional analytical evidence, its composition cannot be assigned specifically to carbon, sulfur, chloride, volatile matter, or unidentified mineral phases.

The major-oxide profiles demonstrate clear compositional differentiation among the three carbonaceous materials. AC displayed a comparatively Si–Al-associated profile, SDC exhibited stronger Ca–Mg–Fe contributions, and RHC was characterized by a pronounced Si–K–P signature. These distinctions establish that the three materials are not chemically equivalent and provide the basis for the grouped oxide analysis.

3.2 Selected Oxide Groupings and Compositional Signatures

The compositional differences identified from the individual major oxides were further examined using selected oxide groupings to clarify broader inorganic patterns among activated carbon (AC), sawdust-derived carbon (SDC), and rice-husk-derived carbon (RHC) (Table 2; Figure 3). The groupings were calculated directly from the measured oxide concentrations and are used here as descriptive compositional indicators rather than as mineral-phase assignments or adsorption-performance indices.

Table 2. Selected major-oxide groupings of activated carbon, sawdust-derived carbon, and rice-husk-derived carbon.

Selected oxide grouping	AC (wt.%)	SDC (wt.%)	RHC (wt.%)
CaO + MgO	5.58	8.49	6.23
Fe_2O_3 + Al_2O_3	5.57	5.10	3.62
CaO + MgO + Fe_2O_3 + Al_2O_3	11.15	13.59	9.85
K_2O + Na_2O	4.57	6.95	8.20
K_2O + P_2O_5	4.98	7.65	9.27

The CaO + MgO fraction was highest in SDC at 8.49 wt.%, compared with 5.58 wt.% in AC and 6.23 wt.% in RHC. Thus, the combined Ca–Mg-associated oxide fraction in SDC was approximately 52.2% higher than that of AC and 36.3% higher than that of RHC. A similar pattern emerged when CaO, MgO, Fe_2O_3, and Al_2O_3 were considered together. This combined fraction reached 13.59 wt.% in SDC, compared with 11.15 wt.% in AC and 9.85 wt.% in RHC, corresponding to approximately 21.9% and 38.0% higher values, respectively. These results reinforce the Ca–Mg–Fe-enriched compositional profile identified for SDC in Section 3.1.

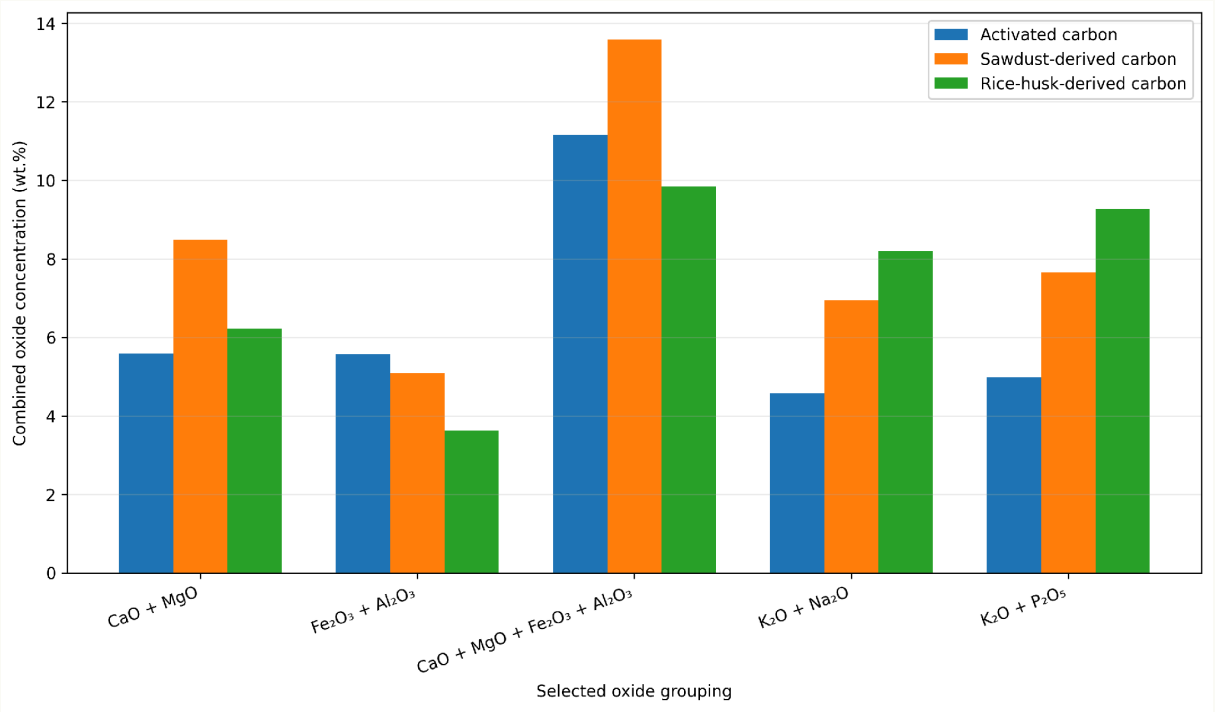

Figure 3. Selected oxide groupings of activated carbon, sawdust-derived carbon, and rice-husk-derived carbon.

In contrast, the combined $Fe_2O_3 + Al_2O_3$ fraction was highest in AC (5.57 wt.%), followed closely by SDC (5.10 wt.%) and then RHC (3.62 wt.%). The AC value was approximately 9.2% higher than that of SDC and 53.9% higher than that of RHC. This pattern is consistent with the comparatively high Al_2O_3 concentration observed in AC and further distinguishes its inorganic composition from the K- and P-enriched profile of RHC.

The alkali-associated grouping displayed a different material ordering. The combined $K_2O + Na_2O$ concentration increased from 4.57 wt.% in AC to 6.95 wt.% in SDC and 8.20 wt.% in RHC. The RHC value was therefore approximately 79.4% higher than that of AC and 18.0% higher than that of SDC. Similarly, $K_2O + P_2O_5$ increased from 4.98 wt.% in AC to 7.65 wt.% in SDC and 9.27 wt.% in RHC. The corresponding RHC value was approximately 86.1% higher than AC and 21.2% higher than SDC. These results provide additional quantitative support for the Si–K–P-associated signature of RHC described in Section 3.1.

The grouped oxide profiles are broadly consistent with the established influence of feedstock origin and thermal-processing history on the inorganic composition of carbonaceous materials. Carbon-based sorbents produced from different precursors can retain markedly different proportions of Ca-, Mg-, Fe-, Al-, K-, P-, and Si-containing constituents (Marzeddu et al., 2022). Rice-husk-derived materials in particular are commonly characterized by a silica-rich mineral fraction accompanied by varying amounts of alkali and nutrient-associated constituents, including K and P (Karam et al., 2022; Russo et al., 2023; Taiye et al., 2024). The comparatively large $K_2O + Na_2O$ and $K_2O + P_2O_5$ fractions observed in RHC are therefore consistent with the broader compositional characteristics reported for thermally converted rice residues.

The stronger Ca–Mg-associated profile of SDC may also be relevant when comparing carbonaceous materials for environmental applications. Ca- and Mg-bearing constituents have been associated in previous studies with aqueous contaminant interactions through mechanisms such as ion exchange, surface complexation, and, under suitable solution conditions, precipitation reactions. Fe- and Al-bearing components may likewise provide reactive sites for interaction with dissolved species (Jellali et al., 2024; Srivastav et al., 2024). These literature-reported mechanisms provide a rationale for considering such

constituents during preliminary adsorbent screening; however, they were not directly demonstrated in the present dataset. Accordingly, the larger Ca–Mg–Fe–Al fraction in SDC should be interpreted as a compositional characteristic rather than evidence of superior adsorption capacity.

Although the analytical results are expressed conventionally as CaO, MgO, Fe_2O_3, Al_2O_3, K_2O, and other oxide equivalents, these values do not establish that the elements occur in the samples as discrete crystalline oxide phases. Calcium, for example, may occur in carbonates, phosphates, silicates, or other mineral associations, depending on feedstock composition and thermal history. Confirming specific mineral phases would require independent mineralogical characterization.

The grouped oxide analysis strengthens the differentiation among the three materials. SDC exhibited the highest CaO + MgO and CaO + MgO + Fe_2O_3 + Al_2O_3 fractions, AC showed the highest Fe_2O_3 + Al_2O_3 grouping, and RHC had the largest K_2O + Na_2O and K_2O + P_2O_5 fractions. These patterns reinforce the broader compositional signatures of Si–Al for AC, Ca–Mg–Fe for SDC, and Si–K–P for RHC.

3.3 Trace-Element Profiles of the Carbonaceous Materials

The trace-element concentrations further differentiated activated carbon (AC), sawdust-derived carbon (SDC), and rice-husk-derived carbon (RHC) (Table 3). Thirteen elements were quantified, namely Ba, Cu, Cr, Ni, Zn, Co, Sr, Pb, Sc, Cd, Nb, Rb, and Zr. Considerable variation was observed among individual elements and materials. SDC recorded the highest concentrations for 10 of the 13 measured trace elements, whereas RHC recorded the highest concentrations of Ba, Sr, and Rb. None of the measured trace elements reached its maximum concentration in AC.

Table 3. Trace-element concentrations of activated carbon, sawdust-derived carbon, and rice-husk-derived carbon.

Element	AC (mg kg^{-1})	SDC (mg kg^{-1})	RHC (mg kg^{-1})
Ba	318.6	186.4	527.8
Cu	8.7	14.2	11.6
Cr	5.8	8.4	7.1
Ni	6.3	10.7	8.9
Zn	24.5	31.8	27.4
Co	3.2	5.6	4.1
Sr	18.7	25.3	34.6
Pb	3.8	6.5	5.2
Sc	2.1	3.4	2.8
Cd	0.18	0.31	0.12
Nb	0.7	1.1	0.8
Rb	4.6	8.2	11.5
Zr	2.9	4.7	3.6

Among the measured elements, Ba occurred at the highest concentration in each material, ranging from 186.4 mg kg^{-1} in SDC to 527.8 mg kg^{-1} in RHC. RHC contained approximately 2.83 times the Ba concentration measured in SDC and approximately 1.66 times that measured in AC. Zn represented the next most abundant measured trace element, with concentrations of 24.5, 31.8, and 27.4 mg kg^{-1} in AC, SDC, and RHC, respectively. Sr concentrations ranged from 18.7 mg kg^{-1} in AC to 34.6 mg kg^{-1} in RHC,

while the remaining elements generally occurred at concentrations below 15 mg kg^{-1}.

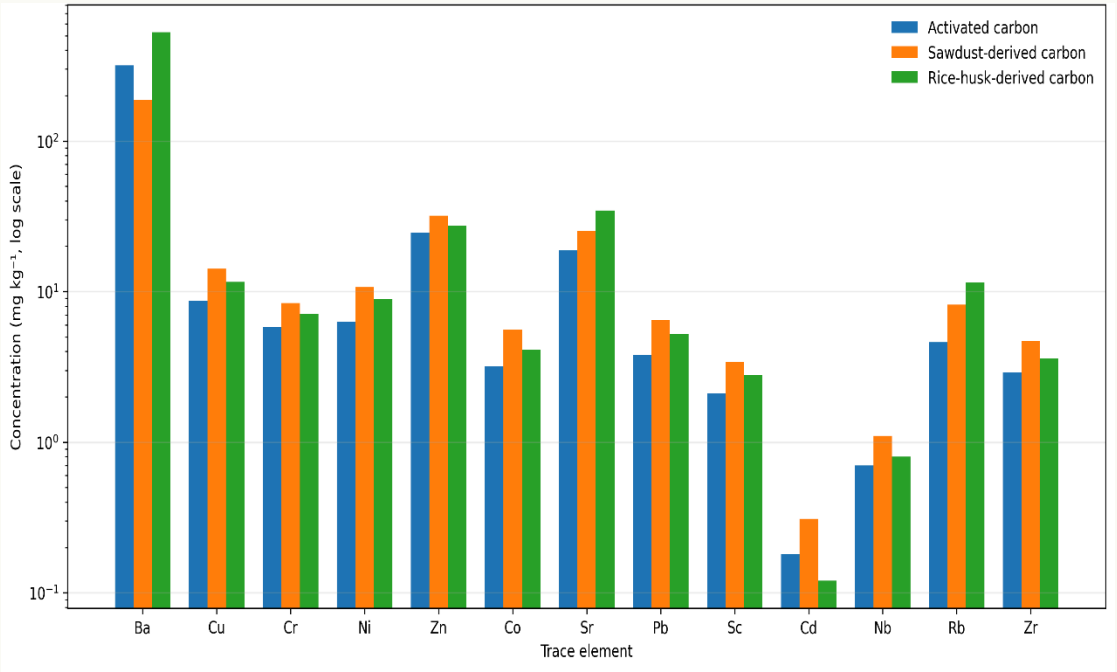

Figure 4. Trace-element concentrations of activated carbon, sawdust-derived carbon, and rice-husk-derived carbon (logarithmic y-axis).

The trace-element profile of SDC was characterized by comparatively high concentrations across a broad range of elements. SDC recorded the highest Cu (14.2 mg kg^{-1}), Cr (8.4 mg kg^{-1}), Ni (10.7 mg kg^{-1}), Zn (31.8 mg kg^{-1}), Co (5.6 mg kg^{-1}), Pb (6.5 mg kg^{-1}), Sc (3.4 mg kg^{-1}), Cd (0.31 mg kg^{-1}), Nb (1.1 mg kg^{-1}), and Zr (4.7 mg kg^{-1}) concentrations. By comparison, AC consistently showed lower concentrations than SDC for these ten elements, while RHC generally exhibited intermediate values, except for Cd, for which RHC recorded the lowest concentration (0.12 mg kg^{-1}). These results define SDC as the material with the broadest relative enrichment across the measured transition and trace-element suite.

RHC exhibited a different elemental pattern, characterized by comparatively high Ba, Sr, and Rb concentrations. Ba reached 527.8 mg kg^{-1} in RHC, compared with 318.6 mg kg^{-1} in AC and 186.4 mg kg^{-1} in SDC. Sr similarly increased from 18.7 mg kg^{-1} in AC to 25.3 mg kg^{-1} in SDC and 34.6 mg kg^{-1} in RHC. Rb followed the same ordering, increasing from 4.6 mg kg^{-1} in AC to 8.2 mg kg^{-1} in SDC and 11.5 mg kg^{-1} in RHC. Relative to AC, the RHC concentrations were approximately 1.66 times higher for Ba, 1.85 times higher for Sr, and 2.50 times higher for Rb. The simultaneous enrichment of these three elements therefore distinguishes RHC from the broader transition-metal enrichment observed in SDC.

The material-specific distributions observed here are consistent with the broader understanding that the trace-element composition of carbonaceous materials reflects both the elemental composition of the precursor and changes that occur during thermal conversion. Pyrolysis and related carbonization processes remove substantial quantities of volatile organic matter while retaining many non-volatile inorganic constituents, which can result in their relative concentration in the solid product. At the same time, the extent of enrichment depends on feedstock chemistry, processing temperature, mineral transformations, washing, and post-treatment conditions. Comparative characterization studies have therefore reported substantial heterogeneity in the elemental composition of carbonaceous sorbents prepared from different precursors (Marzeddu et al., 2022; Karam et al., 2022; Russo et al., 2023).

The relatively high Ba–Sr–Rb signature of RHC is also compatible with the distinct inorganic chemistry of rice-derived biomass. Rice-husk-derived materials are well known to retain substantial inorganic matter

during thermal conversion, although most previous studies have emphasized silica and major ash-forming constituents rather than the complete trace-element suite (Hossain et al., 2020; Karam et al., 2022; Taiye et al., 2024). The present results extend that compositional characterization by showing that, within the measured element set, RHC was distinguished not only by its Si–K–P major-oxide profile but also by comparatively high Ba, Sr, and Rb concentrations. The data do not establish the chemical forms or mineral hosts of these elements, so their association with specific phases should not be inferred without additional mineralogical evidence.

The broad trace-element enrichment observed in SDC likewise should be interpreted as a characteristic of the investigated material rather than a universal property of sawdust-derived carbon. Feedstock source can substantially influence the initial concentrations of Cu, Zn, Ni, Cr, Pb, and other elements, while processing can further alter their concentrations in the resulting carbonaceous material. Recent reviews and environmental assessments emphasize that such variability is an important consideration when characterizing biochar and related sorbents for environmental use (Das, 2024; Dong et al., 2025; Danesh et al., 2025). Consequently, material identity alone is insufficient to predict trace-element composition; direct chemical characterization remains necessary.

Importantly, the concentrations as shown in Table 3 represent total solid-phase concentrations expressed in mg kg^{-1}. They do not indicate the fraction that is soluble, mobile, bioavailable, or capable of being released into water. The presence of a trace element in the solid material therefore cannot be equated directly with environmental exposure or leaching risk. This distinction is particularly important for carbonaceous materials intended for environmental applications, where total elemental inventory and elemental mobility represent related but separate properties (Marcińczyk et al., 2024; Dong et al., 2025).

Overall, the trace-element results reveal two contrasting compositional patterns. SDC exhibited the highest concentrations of 10 of the 13 measured elements, including Cu, Cr, Ni, Zn, Co, Pb, Sc, Cd, Nb, and Zr, whereas RHC was distinguished by the highest Ba, Sr, and Rb concentrations. AC did not exhibit the maximum concentration for any measured trace element and generally showed a comparatively lower trace-element profile.

3.4 Environmentally Relevant Trace Elements

The trace-element dataset was further examined with emphasis on Cu, Cr, Ni, Zn, Pb, and Cd because these elements are commonly considered in environmental assessment and in the evaluation of materials intended for water-treatment and remediation applications. Their concentrations differed among activated carbon (AC), sawdust-derived carbon (SDC), and rice-husk-derived carbon (RHC), with SDC recording the highest concentration for each of the six elements considered (Table 4).

Table 4. Concentrations and inter-material contrasts of selected environmentally relevant trace elements in activated carbon, sawdust-derived carbon, and rice-husk-derived carbon.

Element	AC (mg kg^{-1})	SDC (mg kg^{-1})	RHC (mg kg^{-1})	Highest material	Max/min ratio
Cu	8.70	14.20	11.60	SDC	1.63
Cr	5.80	8.40	7.10	SDC	1.45
Ni	6.30	10.70	8.90	SDC	1.70
Zn	24.50	31.80	27.40	SDC	1.30
Pb	3.80	6.50	5.20	SDC	1.71

Element	AC (mg kg⁻¹)	SDC (mg kg⁻¹)	RHC (mg kg⁻¹)	Highest material	Max/min ratio
Cd	0.18	0.31	0.12	SDC	2.58

Among these elements, Zn occurred at the highest absolute concentration, ranging from 24.5 mg kg⁻¹ in AC to 31.8 mg kg⁻¹ in SDC, followed by Cu, Ni, Cr, Pb, and Cd. Relative to AC, SDC contained approximately 63.2% more Cu, 44.8% more Cr, 69.8% more Ni, 29.8% more Zn, 71.1% more Pb, and 72.2% more Cd. AC recorded the lowest concentrations of Cu, Cr, Ni, Zn, and Pb, whereas the lowest Cd concentration occurred in RHC (0.12 mg kg⁻¹). The largest proportional contrast among the six elements was observed for Cd, for which the maximum-to-minimum concentration ratio was 2.58, followed by Pb (1.71), Ni (1.70), Cu (1.63), Cr (1.45), and Zn (1.30).

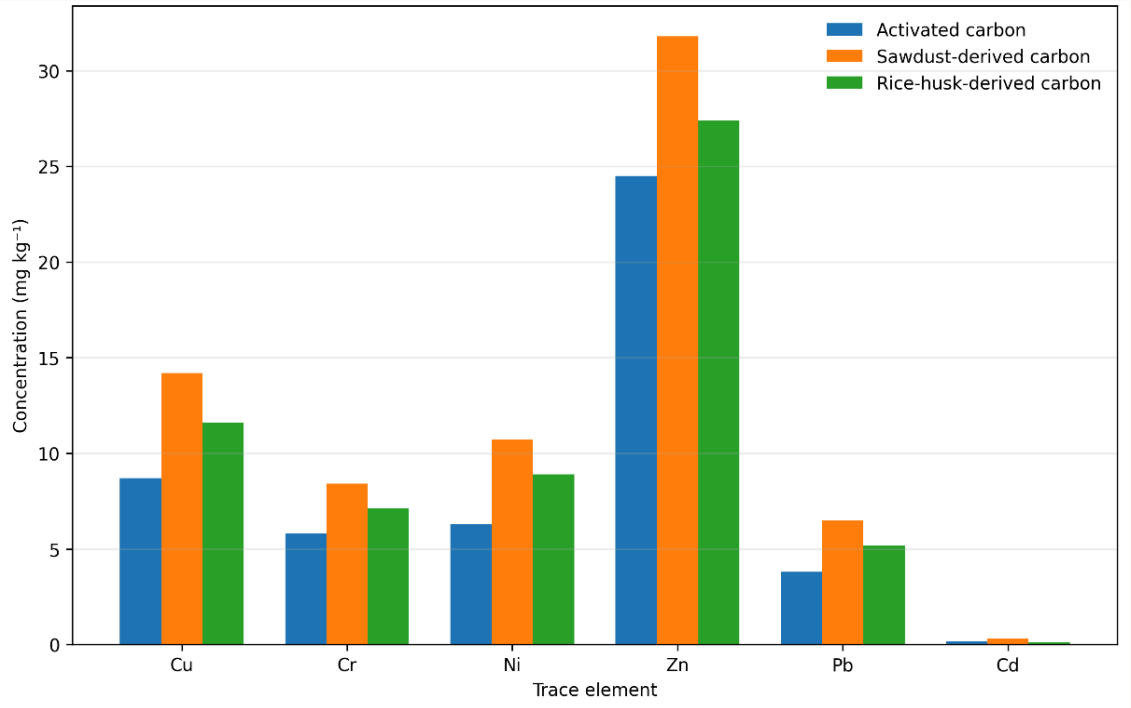

Figure 5. Concentrations of selected environmentally relevant trace elements in activated carbon, sawdust-derived carbon, and rice-husk-derived carbon.

The consistent enrichment of Cu, Cr, Ni, Zn, Pb, and Cd in SDC provides an important additional dimension to the compositional differences identified from the major oxides. While Section 3.2 showed that SDC possessed the highest combined Ca–Mg and Ca–Mg–Fe–Al oxide fractions, the present results show that the same material also contained the largest solid-phase inventory of the six selected environmentally relevant trace elements. This finding does not necessarily indicate environmental unsuitability, but it demonstrates why trace-element composition should be considered alongside potentially beneficial mineral constituents when screening carbonaceous materials for environmental use.

Such material-to-material variability is consistent with the broader biochar literature. The concentrations of trace elements retained in carbonaceous products depend strongly on the elemental composition of the original feedstock and on thermal-processing conditions. During carbonization, loss of organic matter can increase the relative concentration of comparatively non-volatile inorganic constituents, although individual elements may also undergo transformation, redistribution, volatilization, or stabilization depending on temperature and mineral association. Consequently, carbonaceous materials prepared from different precursors can exhibit markedly different trace-element inventories even when they are intended for similar environmental applications (Marzeddu et al., 2022; Karam et al., 2022; Russo et al., 2023;

Dong et al., 2025).

The environmental relevance of the six elements also differs according to their chemical behavior. Cu and Zn are essential micronutrients at appropriate concentrations but can become environmentally undesirable when present at excessive levels, whereas Pb and Cd are generally regarded as potentially toxic elements of particular concern. Cr and Ni likewise require attention because their environmental behavior and toxicity depend on concentration, chemical form, oxidation state, and exposure conditions. Recent reviews of biochar and related adsorbents therefore emphasize that environmental performance should be assessed not solely from contaminant-removal capacity but also from the chemical composition and safety of the adsorbent itself (Zeng et al., 2024; Srivastav et al., 2024; Dong et al., 2025; Ahmed & Aidi, 2025).

The higher solid-phase concentrations observed in SDC is not evidence that these elements would be released into treated water. The values in Table 4 are expressed as: mg kg^{-1} of solid material, whereas concentrations in water are normally expressed as:mg L^{-1} or µg L^{-1}

These units describe fundamentally different quantities and cannot be compared directly. More importantly, total elemental concentration does not establish the soluble, exchangeable, mobile, or leachable fraction of an element. Element mobility depends on factors including mineral association, oxidation state, solution pH, ionic strength, contact time, and the physicochemical structure of the carbonaceous material. Recent work on environmental safety of biochar similarly distinguishes total trace-element inventory from actual mobility and emphasizes that leaching behavior is a separate property that must be evaluated independently when environmental exposure is the research question (Dong et al., 2025; Rehman et al., 2025).

The measured values therefore provide a basis for compositional screening as the Pb concentration of 6.5 mg kg^{-1} in SDC establishes that SDC contained more Pb than AC (3.8 mg kg^{-1}) and RHC (5.2 mg kg^{-1}), but it does not indicate the concentration of Pb that would occur in water contacting the material. Similarly, the Cd concentration of 0.31 mg kg^{-1} in SDC cannot be converted directly into an aqueous exposure concentration.

The relative differences among the materials nevertheless remain relevant to adsorbent selection. A candidate water-treatment material may possess mineral constituents that are potentially favorable for contaminant interactions while simultaneously containing an intrinsic inventory of environmentally relevant elements. Material screening should therefore consider both characteristics. In this study, SDC combines the strongest Ca–Mg–Fe-associated oxide profile with the highest concentrations of the six selected environmentally relevant trace elements, whereas AC generally contains the lowest concentrations of Cu, Cr, Ni, Zn, and Pb. RHC occupies an intermediate position for these five elements and contains the lowest Cd concentration.

The selected trace-element analysis demonstrates that the three carbonaceous materials differ not only in their major-oxide chemistry but also in their intrinsic inventories of environmentally relevant elements. SDC showed the highest Cu, Cr, Ni, Zn, Pb, and Cd concentrations, with the greatest inter-material proportional contrast observed for Cd. These differences are relevant to preliminary material screening but do not constitute evidence of trace-element mobility, leaching, or water-quality impact.

3.5 Inter-Material Compositional Contrast

To identify the chemical variables that most strongly differentiated activated carbon (AC), sawdust-derived carbon (SDC), and rice-husk-derived carbon (RHC), the inter-material contrast for each measured parameter was expressed as the ratio between its maximum and minimum concentration:

$$CR = Cmax / Cmin$$

where CR is the concentration contrast ratio and Cmax and Cmin are the highest and lowest values recorded among the three materials, respectively. A ratio approaching 1 indicates relatively little variation among the materials, whereas progressively larger ratios indicate greater compositional contrast. The ratios are used strictly as descriptive measures and should not be interpreted as statistical effect sizes or evidence of significant differences.

Table 5. Inter-material concentration contrasts for the major oxides and trace elements measured in activated carbon, sawdust-derived carbon, and rice-husk-derived carbon.

Parameter	Maximum	Material	Minimum	Material	Max/min ratio
Ba (mg kg^{-1})	527.80	RHC	186.40	SDC	**2.83**
MnO (wt.%)	0.24	RHC	0.09	AC	**2.67**
Cd (mg kg^{-1})	0.31	SDC	0.12	RHC	**2.58**
Rb (mg kg^{-1})	11.50	RHC	4.60	AC	**2.50**
MgO (wt.%)	2.86	SDC	1.31	RHC	**2.18**
Fe_2O_3 (wt.%)	1.92	SDC	0.88	RHC	**2.18**
P_2O_5 (wt.%)	1.43	RHC	0.72	AC	**1.99**
Sr (mg kg^{-1})	34.60	RHC	18.70	AC	**1.85**
K_2O (wt.%)	7.84	RHC	4.26	AC	**1.84**
Co (mg kg^{-1})	5.60	SDC	3.20	AC	**1.75**
TiO_2 (wt.%)	0.31	RHC	0.18	AC	**1.72**
Pb (mg kg^{-1})	6.50	SDC	3.80	AC	**1.71**
Ni (mg kg^{-1})	10.70	SDC	6.30	AC	**1.70**
Cu (mg kg^{-1})	14.20	SDC	8.70	AC	**1.63**
Zr (mg kg^{-1})	4.70	SDC	2.90	AC	**1.62**
Sc (mg kg^{-1})	3.40	SDC	2.10	AC	**1.62**
Nb (mg kg^{-1})	1.10	SDC	0.70	AC	**1.57**
Na_2O (wt.%)	0.48	SDC	0.31	AC	**1.55**
Al_2O_3 (wt.%)	4.21	AC	2.74	RHC	**1.54**
CaO (wt.%)	5.63	SDC	3.84	AC	**1.47**
Cr (mg kg^{-1})	8.40	SDC	5.80	AC	**1.45**
SiO_2 (wt.%)	73.18	RHC	54.76	SDC	**1.34**
Zn (mg kg^{-1})	31.80	SDC	24.50	AC	**1.30**

The largest contrast among the individually identified parameters was observed for Ba, with a maximum-to-minimum ratio of 2.83. RHC contained 527.8 mg kg^{-1} Ba, compared with 186.4 mg kg^{-1} in SDC. Among the measured oxides, MnO showed the greatest contrast, with a ratio of 2.67, reflecting concentrations of 0.24 wt.% in RHC and 0.09 wt.% in AC. Cd and Rb also displayed pronounced inter-material differences, with contrast ratios of 2.58 and 2.50, respectively. SDC recorded the maximum Cd concentration, whereas RHC contained the highest Rb concentration.

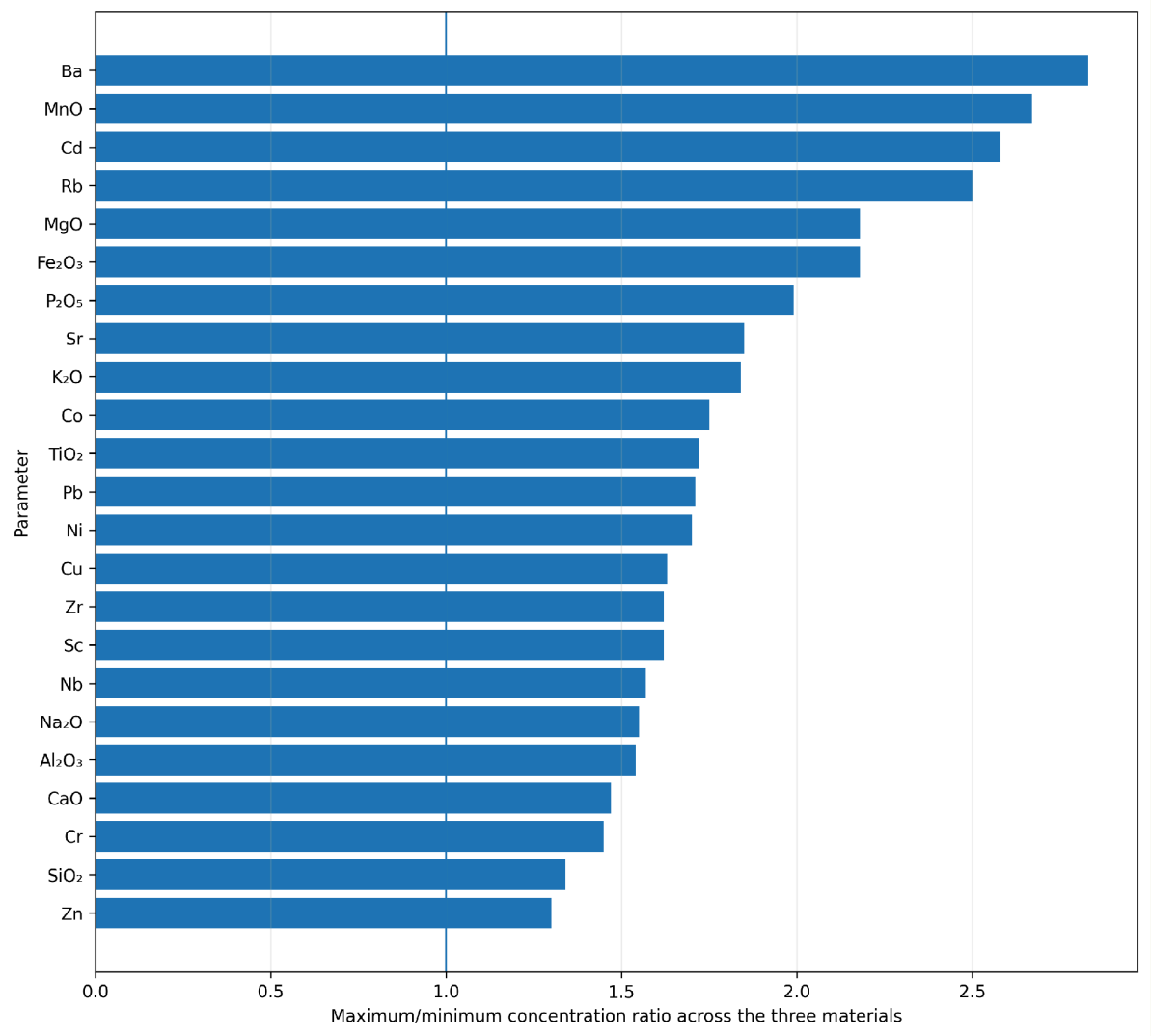

Figure 6. Inter-material compositional contrast based on maximum-to-minimum concentration ratios for identified major oxides and trace elements; the Other/undetermined fraction is excluded.

Several of the major oxides that defined the material-specific signatures also exhibited relatively large contrast ratios. MgO and Fe_2O_3 each varied by approximately 2.18-fold across the three materials, with maxima in SDC and minima in RHC. P_2O_5 showed a ratio of 1.99, while K_2O varied by a factor of 1.84, with RHC recording the maximum concentration for both oxides. These contrasts reinforce the distinction between the comparatively Ca–Mg–Fe-associated composition of SDC and the Si–K–P-associated composition of RHC.

An important feature of the results is that the most abundant constituent was not necessarily the most variable. SiO_2 dominated the reported major-oxide composition of all three materials, yet its inter-material contrast ratio was only 1.34, considerably lower than those of MnO, MgO, Fe_2O_3, P_2O_5, and K_2O. Thus, while SiO_2 accounted for the largest proportion of the reported inorganic composition, several lower-abundance oxides provided greater proportional discrimination among the three materials. This distinction is important because compositional differentiation should not be evaluated solely from the most abundant constituent.

A similar pattern occurred within the trace-element dataset. Ba, Cd, and Rb showed the strongest proportional contrasts, whereas Zn, the second most abundant measured trace element after Ba displayed the smallest trace-element contrast, with a ratio of only 1.30. Pb, Ni, Cu, Co, Zr, Sc, and Nb showed intermediate ratios ranging from approximately 1.57 to 1.75. These results indicate that elements occurring

at relatively low absolute concentrations can nevertheless contribute strongly to differentiating carbonaceous materials when their relative variation among samples is considered.

The pattern of inter-material variability is consistent with the broader understanding that carbonaceous materials inherit chemically distinct inorganic inventories from their precursor feedstocks and that these inventories can subsequently be modified by thermal processing. Comparative characterization studies have repeatedly demonstrated that feedstock type, pyrolysis temperature, activation, washing, and post-treatment influence the retention and concentration of mineral and trace-element constituents in biochar and activated carbon (Karam et al., 2022; Marzeddu et al., 2022; Russo et al., 2023). More recent reviews similarly emphasize that biochar composition should be considered material-specific rather than assumed from the general feedstock category alone (Taiye et al., 2024; Matarru & Shin, 2025; Danesh et al., 2025).

The relatively strong variation in MgO, Fe_2O_3, P_2O_5, and K_2O is therefore compatible with differences in biomass mineral composition and thermal history. However, the present dataset does not permit the relative contributions of feedstock and processing conditions to be separated quantitatively. Likewise, the observed Ba, Cd, and Rb contrasts establish differences in total solid-phase concentrations but do not identify the processes responsible for those differences. Attribution to specific mineral phases, volatilization behavior, or feedstock uptake pathways would require additional evidence. The contrast ratios should therefore be interpreted as empirical measures of differentiation, not mechanistic explanations.

This distinction is particularly relevant when considering adsorbent selection. Chemical variables with high contrast ratios may help distinguish candidate materials and identify properties requiring closer consideration, but a large contrast ratio does not imply that an element or oxide controls adsorption performance. For example, the 2.18-fold contrast in MgO or the 1.99-fold contrast in P_2O_5 may be relevant to hypotheses concerning mineral-mediated interactions with aqueous contaminants, because Mg-, Ca-, Fe-, Al-, and P-bearing materials have been implicated in contaminant retention in previous studies. Such mechanisms, however, depend on mineral form, surface accessibility, solution chemistry, and adsorbate identity and cannot be inferred from concentration ratios alone (Jellali et al., 2024; Kumar et al., 2025).

The contrast analysis also provides an environmental-screening perspective. SDC exhibited maxima for Cd, Pb, Ni, Cu, Co, and several other trace elements, whereas RHC exhibited maxima for Ba, Sr, and Rb. Recent literature on safe environmental application of biochar emphasizes that heterogeneity in intrinsic inorganic and trace-element composition should be considered when evaluating carbonaceous materials for environmental use (Dong et al., 2025

The inter-material contrast analysis confirms that compositional differentiation among AC, SDC, and RHC is distributed across both major oxides and trace elements rather than being controlled by a single constituent. The strongest contrasts among identified parameters occurred for Ba, MnO, Cd, Rb, MgO, and Fe_2O_3, while SiO_2 and Zn showed comparatively smaller proportional variation despite their relatively high absolute concentrations.

3.6 Analytical Precision of SiO_2 Determination

Analytical precision for SiO_2 was assessed using the relative standard deviation (RSD) of the replicate measurements. The RSD values were 1.8% for activated carbon (AC), 2.4% for sawdust-derived carbon (SDC), and 1.6% for rice-husk-derived carbon (RHC) (Table 6). Thus, the observed RSD values ranged from 1.6 to 2.4%, with RHC showing the lowest relative variability and SDC the highest. All three values were below 2.5%, indicating relatively low dispersion among the replicate SiO_2 measurements.

Table 6. SiO_2 concentrations and analytical relative standard deviations for activated carbon, sawdust-derived carbon, and rice-husk-derived carbon.

Material	SiO_2 (wt.%)	RSD (%)
Activated carbon (AC)	68.42	1.8
Sawdust-derived carbon (SDC)	54.76	2.4
Rice-husk-derived carbon (RHC)	73.18	1.6

RSD, relative standard deviation; n = 2 analytical measurements per material.

Relative standard deviation expresses analytical variability relative to the magnitude of the measured value and is commonly used to describe precision under repeatability or within-laboratory conditions. Lower RSD values indicate less relative dispersion among replicate measurements, although acceptable precision should ultimately be judged in relation to the analytical method, analyte concentration, measurement conditions, and predefined quality-control criteria (Thompson et al., 2002; Noh & Myung, 2024). Within the present dataset, the narrow RSD range indicates relatively low within-sample analytical variability in the duplicate SiO_2 measurements.

The lowest RSD was obtained for RHC (1.6%), followed by AC (1.8%) and SDC (2.4%). The difference between the highest and lowest RSD values was therefore 0.8 percentage points. Although SDC displayed greater relative variability than AC and RHC, its RSD remained below 2.5%. The data therefore do not indicate pronounced analytical dispersion in the SiO_2 measurements.

These precision results strengthen confidence that the reported SiO_2 concentrations were not based on highly variable replicate measurements. However, RSD should not be interpreted as evidence of analytical accuracy. Precision and trueness represent different components of analytical performance: a method may generate closely grouped replicate values while still exhibiting systematic bias. Evaluation of accuracy or trueness would require additional information such as certified reference materials, recovery experiments, calibration performance, or comparison with an independent reference method (Thompson et al., 2002; Murphy et al., 2013; Noh & Myung, 2024). Such information is not contained in the present dataset and is therefore not inferred.

Similarly, the RSD values do not provide a statistical test of the differences in SiO_2 concentration among AC, SDC, and RHC. Although the measured concentrations differed substantially with 54.76 wt.% in SDC, 68.42 wt.% in AC, and 73.18 wt.% in RHC, the duplicate analytical measurements do not constitute independent replicate material batches suitable for population-level inferential testing. The oxide differences can be described as observed compositional differences rather than statistically significant differences. (Thompson et al., 2002; Sharma et al., 2021; Noh & Myung, 2024).

The 1.6–2.4% RSD range indicates relatively consistent replicate SiO_2 measurements across the three carbonaceous materials and provides useful quality-control support for the principal oxide reported in the study. At the same time, the RSD results show strictly as evidence of analytical precision and proof of accuracy for the remaining analytes.

3.7 Implications of Major-Oxide Composition for Adsorbent Selection

The major-oxide results demonstrate that activated carbon (AC), sawdust-derived carbon (SDC), and rice-husk-derived carbon (RHC) possess chemically distinct inorganic profiles that may be relevant to their preliminary assessment as water-treatment adsorbents. As shown in Table 2 and Figure 3, SDC contained the highest combined CaO + MgO fraction (8.49 wt.%) and the highest CaO + MgO + Fe_2O_3 + Al_2O_3 fraction (13.59 wt.%). AC displayed the highest Fe_2O_3 + Al_2O_3 grouping (5.57 wt.%), whereas RHC was

distinguished by the highest $K_2O + Na_2O$ (8.20 wt.%) and $K_2O + P_2O_5$ (9.27 wt.%) fractions in addition to its high SiO_2 concentration (73.18 wt.%). These differences indicate that the three materials may provide different inorganic chemical environments for interaction with aqueous contaminants. However, the oxide concentrations represent compositional characteristics and should not be interpreted as direct measurements of adsorption capacity or contaminant-removal efficiency.

The comparatively high Ca- and Mg-associated fraction of SDC may be relevant to adsorbent screening because Ca- and Mg-bearing components have been associated with contaminant retention in a range of biochar-based materials. Depending on contaminant identity and solution chemistry, reported mechanisms include ion exchange, surface complexation, and precipitation or co-precipitation involving mineral constituents (Ahmad et al., 2014; Mohan et al., 2014; Tan et al., 2015). More recent studies involving mineral-modified biochars have similarly demonstrated that Mg- and Ca-containing components can contribute to the retention of dissolved species, particularly phosphate and selected metal ions, under suitable chemical conditions (Jellali et al., 2024). The 8.49 wt.% CaO + MgO fraction observed in SDC therefore provides a compositional reason for considering mineral-associated interactions during preliminary adsorbent assessment. Nevertheless, these mechanisms have not been demonstrated directly for the present SDC sample and should be treated as literature-supported possibilities rather than experimentally confirmed processes.

Fe- and Al-associated constituents may also be relevant to contaminant retention because Fe- and Al-bearing surfaces can interact with dissolved species through mechanisms including ligand exchange, surface complexation, electrostatic interaction, and, under some conditions, precipitation or co-precipitation. AC showed the largest $Fe_2O_3 + Al_2O_3$ grouping at 5.57 wt.%, followed by SDC at 5.10 wt.% and RHC at 3.62 wt.%. This comparatively strong Fe–Al-associated component may therefore contribute to differences in the chemical environments presented by the three materials. However, oxide-equivalent concentrations alone do not establish that Fe and Al occur as discrete Fe_2O_3 or Al_2O_3 mineral phases, nor do they establish whether such constituents are exposed at the adsorbent surface. Mineral form, crystallinity, distribution, and surface accessibility are important determinants of reactivity. Consequently, the Fe–Al grouping should be regarded as a compositional screening parameter rather than direct evidence of specific adsorption sites or mechanisms.

When CaO, MgO, Fe_2O_3, and Al_2O_3 were considered collectively, SDC showed the highest concentration at 13.59 wt.%, compared with 11.15 wt.% in AC and 9.85 wt.% in RHC. This result reinforces the comparatively Ca–Mg–Fe-enriched character of SDC and suggests that its inorganic fraction differs substantially from that of the more silica- and K-rich RHC. Mineral constituents containing Ca, Mg, Fe, and Al have been implicated in the adsorption or immobilization of inorganic contaminants in previous studies, providing a reasonable basis for considering the SDC composition potentially relevant to adsorbent performance (Liu et al., 2015; Marzeddu et al., 2022; Jellali et al., 2024). Nevertheless, a higher concentration of these constituents does not establish superior adsorption performance because contaminant removal also depends on properties not measured in the present dataset, including specific surface area, pore structure, accessible surface functional groups, surface charge, contaminant speciation, solution pH, ionic strength, and competition from coexisting ions.

RHC displayed a markedly different compositional profile. Its SiO_2 concentration of 73.18 wt.% was the highest among the three materials and was accompanied by comparatively high K_2O and P_2O_5 concentrations. This silica-rich composition is consistent with the established characteristics of rice-husk-derived carbonaceous materials, in which substantial amounts of biogenic silica may be retained following thermal conversion (Karam et al., 2022; Russo et al., 2023; Taiye et al., 2024). Studies of rice-husk-derived sorbents further indicate that inorganic components can form an important part of the

physicochemical structure of these materials and may participate in interactions with dissolved contaminants (Russo et al., 2023). Nevertheless, high bulk SiO_2 concentration should not be equated directly with high adsorption capacity. The present data do not establish silica crystallinity, accessible silanol-group density, specific surface area, pore connectivity, or the fraction of silica exposed at the solid–water interface.

The alkali- and P-associated composition of RHC may also influence its behavior in aqueous systems. RHC contained 8.20 wt.% K_2O + Na_2O and 9.27 wt.% K_2O + P_2O_5, the highest values among the three materials. Alkali and alkaline-earth constituents retained in biochars have been reported to influence ash alkalinity, surface charge, pH response, ion-exchange behavior, and mineral reactivity (Ahmad et al., 2014; Karam et al., 2022). However, bulk K_2O and Na_2O concentrations do not indicate how much K or Na would be released into solution, while the presence of P_2O_5 does not establish phosphorus mobility, phosphate release, or phosphorus-related adsorption behavior. Such effects depend on chemical form, solubility, and accessibility and would require direct investigation before they could be attributed to the present RHC material.

The results therefore illustrate why bulk inorganic composition can assist in preliminary adsorbent screening but cannot independently determine treatment performance. Adsorption by carbonaceous materials is generally controlled by a combination of surface area, pore-size distribution, surface functional groups, aromatic structure, electrostatic properties, ion-exchange capacity, mineral composition, and solution chemistry (Ahmad et al., 2014; Mohan et al., 2014; Tan et al., 2015; Liu et al., 2015). Comparative studies of carbon-based sorbents also show that materials with different feedstocks and processing histories may display substantially different physicochemical characteristics even when they belong to the same general material class (Marzeddu et al., 2022). Consequently, the oxide profiles obtained here provide information about potential inorganic contributions to adsorption but are insufficient to rank AC, SDC, and RHC according to contaminant-removal efficiency.

Adsorbent selection should additionally consider the intrinsic trace-element inventory of the candidate materials. This consideration is particularly relevant for SDC, which combined the highest Ca–Mg–Fe–Al-associated oxide fraction with the highest solid-phase concentrations of Cu, Cr, Ni, Zn, Pb, and Cd among the three materials (Table 4; Figure 5). The coexistence of potentially useful mineral constituents and comparatively elevated trace-element concentrations illustrates that material selection involves more than identifying components that may favor adsorption. Recent assessments of environmental biochar applications emphasize the importance of considering both beneficial functionality and potential unintended chemical risks when selecting materials for environmental use (Dong et al., 2025). In the present case, the higher trace-element concentrations in SDC do not demonstrate leaching or water-quality risk, but they provide an additional compositional criterion that should be considered alongside its Ca–Mg–Fe-associated profile.

From a comparative perspective, each material therefore presents a different inorganic profile relevant to preliminary adsorbent screening. AC combines high SiO_2 with the largest Fe_2O_3 + Al_2O_3 fraction and may consequently be viewed as the most strongly Si–Al-associated of the three materials. SDC exhibits the largest CaO + MgO and CaO + MgO + Fe_2O_3 + Al_2O_3 fractions, giving it the strongest Ca–Mg–Fe-associated character, although it also contains the highest concentrations of several environmentally relevant trace elements. RHC is distinguished by high SiO_2 together with the highest K- and P-associated fractions, producing a pronounced Si–K–P compositional signature. These distinctions indicate different potential chemical contributions to adsorbent behavior but do not establish that one material is inherently superior to the others.

The major-oxide composition provides a useful chemical basis for preliminary differentiation of AC, SDC, and RHC as candidate water-treatment adsorbents. Literature evidence indicates that Ca-, Mg-, Fe-, and Al-bearing components can participate in ion exchange, surface complexation, and precipitation processes under appropriate conditions, while silica and alkali-associated constituents may influence surface and solution chemistry. The present results identify compositional conditions under which such mechanisms may be plausible but do not demonstrate that they occurred in the investigated materials. Accordingly, major-oxide composition should be treated as one component of adsorbent selection, considered together with trace-element inventory and other physicochemical characteristics rather than as a stand-alone predictor of adsorption performance.

3.8 Trace-Element Inventory as an Adsorbent-Selection Criterion

The intrinsic trace-element composition of a carbonaceous material represents an additional consideration when evaluating its suitability for environmental applications. As shown in Tables 3 and 4 and Figures 4 and 5, sawdust-derived carbon (SDC) recorded the highest concentrations of 10 of the 13 measured trace elements, including all six environmentally relevant elements selected for detailed consideration: Cu, Cr, Ni, Zn, Pb, and Cd. Rice-husk-derived carbon (RHC), in contrast, contained the highest concentrations of Ba, Sr, and Rb, while activated carbon (AC) did not record the maximum concentration of any of the measured trace elements. These differences indicate that the three materials possess distinct trace-element inventories in addition to the major-oxide contrasts described previously.

Among the selected environmentally relevant elements, SDC contained 14.2 mg kg^{-1} Cu, 8.4 mg kg^{-1} Cr, 10.7 mg kg^{-1} Ni, 31.8 mg kg^{-1} Zn, 6.5 mg kg^{-1} Pb, and 0.31 mg kg^{-1} Cd. Relative to AC, these concentrations were approximately 63.2%, 44.8%, 69.8%, 29.8%, 71.1%, and 72.2% higher, respectively. The largest proportional difference among these elements occurred for Cd, whose maximum-to-minimum concentration ratio was 2.58. Pb and Ni also showed appreciable inter-material contrasts, with corresponding ratios of 1.71 and 1.70. Consequently, SDC combined the strongest Ca–Mg–Fe-associated oxide profile identified in Sections 3.2 and 3.7 with the highest solid-phase concentrations of several trace elements that warrant consideration in environmental material screening.

This coexistence highlights an important aspect of adsorbent selection. A material may contain mineral constituents that are potentially favorable for contaminant interactions while simultaneously possessing an intrinsic inventory of elements that require environmental consideration. Biochar and other carbonaceous sorbents can retain trace elements originating from their precursor materials, and thermal conversion may alter their relative concentrations through loss of organic matter, mineral transformation, or element-specific retention and volatilization processes (Karam et al., 2022; Marzeddu et al., 2022; Russo et al., 2023). Recent assessments of biochar safety have therefore emphasized that beneficial functionality should be considered together with intrinsic chemical composition and the possibility of unintended contaminant release (Dong et al., 2025).

The lower solid-phase concentrations of Cu, Cr, Ni, Zn, and Pb in AC may be favorable from a compositional-screening perspective when compared with SDC, but these differences should not be interpreted as direct measures of environmental safety. Similarly, the lower Cd concentration in RHC (0.12 mg kg^{-1}) compared with AC (0.18 mg kg^{-1}) and SDC (0.31 mg kg^{-1}) establishes a lower total Cd inventory within the analyzed material but does not establish lower Cd release under aqueous conditions. Total elemental concentration and elemental mobility are related but distinct characteristics.

This distinction is especially important for water-treatment applications. The trace-element concentrations reported in this study are expressed as mg kg^{-1} of solid material, whereas drinking-water and wastewater concentrations are generally expressed as mg L^{-1} or µg L^{-1}. Direct comparison between these values would

therefore be inappropriate. Moreover, only a fraction of the total solid-phase inventory may be soluble or exchangeable under a particular set of aqueous conditions. Release can depend on pH, redox conditions, ionic strength, contact time, mineral association, element speciation, and the physicochemical properties of the carbonaceous matrix. The present data consequently do not establish whether any of the measured elements would be released into water.

The comparatively high Ba concentration in RHC (527.8 mg kg^{-1}) similarly requires careful interpretation. RHC contained approximately 2.83 times as much Ba as SDC and 1.66 times as much as AC, while its Sr and Rb concentrations were also the highest among the three materials. These values provide useful information about the elemental fingerprint of RHC but cannot by themselves establish environmental exposure or treatment suitability. The chemical form and mobility of these elements would need to be known before their practical significance in a water-treatment system could be determined.

Accordingly, the trace-element dataset is most appropriately used as a screening criterion rather than a direct risk assessment. The results identify which candidate materials possess relatively greater or smaller intrinsic elemental inventories and therefore indicate where closer attention may be warranted during material evaluation. This approach is consistent with the increasing emphasis on evaluating both performance and environmental compatibility when considering biochar and related carbonaceous materials for remediation and water-treatment applications (Ahmad et al., 2014; Mohan et al., 2014; Marzeddu et al., 2022; Dong et al., 2025).

The trace-element profiles introduce an important counterbalance to the potentially favorable mineral characteristics. SDC exhibited the strongest Ca–Mg–Fe-associated composition but also the highest concentrations of Cu, Cr, Ni, Zn, Pb, and Cd. AC generally showed lower concentrations of these selected trace elements, while RHC occupied an intermediate position for most of them and contained the lowest Cd concentration.

3.9 Integrated Comparison of the Three Carbonaceous Materials

Integration of the major-oxide, grouped-oxide, trace-element, and analytical-precision results demonstrates that AC, SDC, and RHC possess three distinct compositional profiles rather than representing chemically interchangeable carbonaceous materials. The principal differences can be summarized as a Si–Al-associated profile for AC, a Ca–Mg–Fe-associated profile for SDC, and a Si–K–P-associated profile for RHC. These distinctions are supported not only by individual oxide concentrations but also by the grouped-oxide analysis and trace-element distributions.

The integrated profiles show different compositional strengths and limitations. AC combined high SiO_2 with the largest Fe_2O_3 + Al_2O_3 grouping and generally lower concentrations than SDC for the six environmentally relevant trace elements considered. SDC showed the strongest Ca–Mg–Fe-associated inorganic contribution, including the highest CaO + MgO + Fe_2O_3 + Al_2O_3 fraction, but also the highest concentrations of 10 of the 13 measured trace elements. RHC combined the highest SiO_2, K_2O, and P_2O_5 concentrations with the highest Ba, Sr, and Rb concentrations and the lowest Cd concentration.

The findings show that no single material possesses an unambiguously favorable compositional profile across all measured criteria. SDC contains the strongest Ca–Mg–Fe-associated oxide fraction but also the largest inventory of several environmentally relevant trace elements. AC exhibits a comparatively strong Si–Al-associated profile together with generally lower concentrations of Cu, Cr, Ni, Zn, and Pb. RHC is distinctly silica-, K-, and P-rich and contains the lowest Cd concentration, but it also has the highest Ba, Sr, and Rb concentrations. The compositional advantages and limitations therefore differ according to the criterion considered.

This integrated comparison supports a multi-criteria approach to adsorbent screening. Bulk oxide chemistry can identify potentially reactive inorganic components, while trace-element analysis can reveal intrinsic constituents that may warrant closer environmental consideration. Neither dataset independently establishes adsorption efficiency, contaminant selectivity, or elemental release. Consequently, the value of the present characterization lies primarily in distinguishing the chemical profiles of the three materials and identifying compositional factors that should be considered when selecting carbonaceous adsorbents for specific water-treatment applications.

3.10 Implications for Preliminary Adsorbent Screening

The combined findings provide a chemical basis for preliminary differentiation of AC, SDC, and RHC as candidate adsorbent materials. Rather than identifying a universally superior material, the results indicate that each carbonaceous material possesses a different combination of inorganic characteristics that may become advantageous or limiting depending on the contaminant, solution chemistry, and treatment objective. This distinction is consistent with the broader adsorption literature, which emphasizes that sorbent performance depends on multiple interacting material properties rather than on a single compositional parameter (Ahmad et al., 2014; Mohan et al., 2014; Tan et al., 2015; Liu et al., 2015).

For preliminary screening, SDC is distinguished by the strongest Ca–Mg–Fe-associated oxide profile, AC by a comparatively strong Si–Al-associated profile and generally lower concentrations of several selected trace elements than SDC, and RHC by its pronounced silica- and K–P-associated composition. These differences may be relevant to contaminant-specific hypotheses, but the present dataset does not determine which material would perform best in actual water treatment.

The results also indicate that selection should be contaminant-specific rather than universal. A material whose mineral composition is potentially favorable for one contaminant may not necessarily be optimal for another because adsorption mechanisms differ among cations, oxyanions, nutrients, organic pollutants, and emerging contaminants. Solution pH, ionic strength, competing ions, contaminant concentration, contact time, and surface chemistry may further change relative material performance (Ahmad et al., 2014; Mohan et al., 2014; Tan et al., 2015). Consequently, the present characterization provides a basis for generating informed hypotheses about material suitability rather than as a substitute for contaminant-specific performance measurements.

4. CONCLUSION

This study comparatively characterized the major-oxide and trace-element compositions of activated carbon (AC), sawdust-derived carbon (SDC), and rice-husk-derived carbon (RHC) to identify compositional differences relevant to preliminary adsorbent screening. The results demonstrated that the three carbonaceous materials were chemically distinct rather than compositionally interchangeable.

RHC exhibited the highest SiO_2 concentration (73.18 wt.%) and was further distinguished by comparatively high K_2O and P_2O_5 concentrations, producing a characteristic Si–K–P-associated profile. AC contained 68.42 wt.% SiO_2 and the highest Al_2O_3 concentration (4.21 wt.%), together with the largest $Fe_2O_3 + Al_2O_3$ grouping (5.57 wt.%), supporting a comparatively Si–Al-associated profile. SDC contained the lowest SiO_2 concentration (54.76 wt.%) but the highest CaO (5.63 wt.%), MgO (2.86 wt.%), and Fe_2O_3 (1.92 wt.%) concentrations. Its combined $CaO + MgO + Fe_2O_3 + Al_2O_3$ fraction reached 13.59 wt.%, the highest among the three materials, indicating a comparatively strong Ca–Mg–Fe-associated inorganic profile.

The trace-element results provided an additional basis for differentiation. SDC recorded the highest concentrations of 10 of the 13 measured trace elements, including Cu, Cr, Ni, Zn, Pb, and Cd, whereas

RHC recorded the highest Ba, Sr, and Rb concentrations. AC did not exhibit the maximum concentration of any measured trace element and generally contained lower concentrations of the selected environmentally relevant elements than SDC. These results indicate that potentially favourable inorganic constituents and intrinsic trace-element inventories should be considered together when screening carbonaceous materials for environmental applications.

Inter-material contrast analysis further showed that the strongest proportional differences among identified constituents occurred for Ba, MnO, Cd, Rb, MgO, and Fe_2O_3, demonstrating that lower-abundance constituents can contribute substantially to compositional differentiation even when SiO_2 dominates the bulk inorganic profile. The reported SiO_2 RSD values of 1.6–2.4% indicated relatively low variability among replicate SiO_2 measurements, although equivalent precision information was not available for the remaining analytes.

The findings support the use of major-oxide and trace-element characterization as a preliminary framework for distinguishing candidate carbonaceous adsorbents. SDC showed the strongest Ca–Mg–Fe-associated composition, AC exhibited a comparatively strong Si–Al-associated profile, and RHC was distinguished by its pronounced Si–K–P composition. Accordingly, the findings support composition-based preliminary screening rather than definitive adsorption-performance ranking; direct adsorption and leaching tests would be required to establish treatment performance and environmental release under defined water-contact conditions.

References

Adekunle, A.A.; Familusi, A.O.; Badejo, A.A.; Adeosun, O.J.; Arogundade, S.A.(2020) Characterisation of activated charcoal, sawdust charcoal and rice husk charcoal as adsorbents in water treatment. *Analecta Tech. Szeged.* 2020, *14*, 19–25.

Ahmad, M., Rajapaksha, A. U., Lim, J. E., Zhang, M., Bolan, N., Mohan, D., Vithanage, M., Lee, S. S., & Ok, Y. S. (2014). Biochar as a sorbent for contaminant management in soil and water: A review. Chemosphere, 99, 19–33. *https://doi.org/10.1016/j.chemosphere.2013.10.071*

Ahmed, A., & Aidi, H. (2025). Biochar for heavy metal remediation: Mechanisms, modifications, and environmental applications. Environmental Science and Pollution Research. https://doi.org/10.1007/s11356-025-36886-3

Danesh, P., Prussi, M., Salimbeni, A., Negro, V., & Chiaramonti, D. (2025). Review on biochar upgrading methods for its application in thermochemical conversion processes and critical materials recovery. *Sustainability, 17*(22), 10194. https://doi.org/10.3390/su172210194

Das, S. K. (2024). Agro-waste based biomass residues valorization for effective adsorption of heavy metal. *Environmental Monitoring and Assessment*. https://doi.org/10.1007/s10661-024-13258-x

Dong, M., Jiang, M., He, L., Zhang, Z., Gustave, W., Vithanage, M., Niazi, N. K., Chen, B., Zhang, GX., Wang, H., & He, F. (2025). Challenges in safe environmental applications of biochar: Identifying risks and unintended consequences. Biochar, 7, 12. *https://doi.org/10.1007/s42773-024-00412-4*

Hossain, N., Nizamuddin, S., Griffin, G., Selvakannan, P., Mubarak, N. M., & Mahlia, T. M. I. (2020). Synthesis and characterization of rice husk biochar via hydrothermal carbonization for wastewater treatment and biofuel production. *Scientific Reports, 10*, 18851. https://doi.org/10.1038/s41598-020-75936-3

Jellali, S., Hadroug, S., Al-Sabahi, J., Bekri, I., Al-Raeesi, A., & Hamdi, W. (2024). Synthesis of Mg-, Al-

and Mg/Al-date palm fronds modified biochars: Characterization and investigations on phosphorus adsorption characteristics. Comptes Rendus Chimie. *https://doi.org/10.5802/crchim.329*

Karam, D. S., Nagabovanalli, P., Rajoo, K. S., Ishak, C. F., Abdu, A., Rosli, Z., Muharam, F. M., & Zulperi, D. (2022). An overview on the preparation of rice husk biochar, factors affecting its properties, and its agriculture application. *Journal of the Saudi Society of Agricultural Sciences, 21*(3), 149–159. https://doi.org/10.1016/j.jssas.2021.07.005

Kumar, P., Singhania, R. R., Sumathi, Y., Kurrey, N. K., Chen, C.-W., Patel, A. K., & Dong, C.-D. (2025). Investigating innovative techniques for biochar modification to enhance the removal of heavy metals from aqueous environments: A comprehensive review. *Clean Technologies and Environmental Policy*. https://doi.org/10.1007/s10098-024-02962-4

Liu, W.-J., Jiang, H., & Yu, H.-Q. (2015). Development of biochar-based functional materials: Toward a sustainable platform carbon material. *Chemical Reviews*, *115*(22), 12251–12285. https://doi.org/10.1021/acs.chemrev.5b00195

Marcińczyk, M., Krasucka, P., Duan, W., Pan, B., & Oleszczuk, P. (2024). Effect of zinc-biochar composite aging on its physicochemical and ecotoxicological properties. *Environmental Pollution, 341*, 122856. https://doi.org/10.1016/j.envpol.2023.122856

Marzeddu, S., Décima, M. A., Camilli, L., Bracciale, M. P., Genova, V., Paglia, L., Marra, F., & Boni, M. R. (2022). Physical-chemical characterization of different carbon-based sorbents for environmental applications. *Materials, 15*(20), 7162. https://doi.org/10.3390/ma15207162

Matarru, A. A., & Shin, D. (2025). Biochar production technology as a negative emission strategy: A review. *Energies, 18*(18), 4898. https://doi.org/10.3390/en18184898

Mohan, D., Sarswat, A., Ok, Y. S., & Pittman, C. U., Jr. (2014). Organic and inorganic contaminants removal from water with biochar, a renewable, low-cost and sustainable adsorbent—A critical review. *Bioresource Technology*, *160*, 191–202. https://doi.org/10.1016/j.biortech.2014.01.120

Morales, L. F., Herrera, K., López, J. E., & Saldarriaga, J. F. (2021). Use of biochar from rice husk pyrolysis: Assessment of reactivity in lime pastes. Heliyon, 7, e08423. *https://doi.org/10.1016/j.heliyon.2021.e08423*

Murphy, C. J., MacNeil, J. D., & Capar, S. G. (2013). Best practices for single-laboratory validation of chemical methods for trace elements in foods. Part I—Background and general considerations. *Journal of AOAC International, 96*(1), 190–203. https://academic.oup.com/jaoac/article/96/1/190/5654933

Noh, J., & Myung, S. W. (2024). Understanding and comparative analysis of analytical method validation. *Analytical Science and Technology, 37*(3), 131–140. https://accesson.kr/ast/v.37/3/131/43255

Rehman, H., Khan, A. H. A. , & Rehman, W. U. (2025). Biochar for sustainable restoration of heavy metals contaminated soil: Performance, assessment, and mechanisms. Advanced Sustainable Systems. *https://doi.org/10.1002/adsu.202500776*

Russo, B., Causse, J., Rey, C., Lautru, J., Rebiscoul, D., & Ayral, A. (2023). Biosourced adsorbent prepared with rice husk part 1: A complete understanding of the structure of materials, the major role of mineral impurities for metal extraction. *Sustainable Materials and Technologies, 36*, e00601. https://www.sciencedirect.com/science/article/pii/S2214993723000362

Sharma, A., Dubey, J. K., Katna, S., Shandil, D., Brar, G. S., & Singh, S. (2021). Validation of analytical

methods used for pesticide residue detection in fruits and vegetables. *Food Analytical Methods*. https://doi.org/10.1007/s12161-021-02027-y

Srivastav, A. L., Rani, L., Sharda, P., Patel, A., & Patel, N., (2024). Sustainable biochar adsorbents for dye removal from water: Present state of art and future directions. Adsorption. https://doi.org/10.1007/s10450-024-00522-2

Taiye, M. A., Hafida, W., Kong, F., & Zhou, C. (2024). A review of the use of rice husk silica as a sustainable alternative to traditional silica sources in various applications. *Environmental Progress & Sustainable Energy, 43*(6), e14451. https://doi.org/10.1002/ep.14451

Tan, X., Liu, Y., Zeng, G., Wang, X., Hu, X., Gu, Y., & Yang, Z. (2015). Application of biochar for removal of pollutants from aqueous solutions. *Chemosphere*, *125*, 70–85. https://doi.org/10.1016/j.chemosphere.2014.12.058

Thompson, M., Ellison, S. L. R., & Wood, R. (2002). Harmonized guidelines for single-laboratory validation of methods of analysis. *Pure and Applied Chemistry*, *74*(5), 835–855. https://doi.org/10.1351/pac200274050835

Zeng, Y., Lin, Y., Ma, M., & Chen, H. (2024). A review on the removal of heavy metals from water by phosphorus-enriched biochar. Minerals, 14(1), 61. *https://www.mdpi.com/2075-163X/14/1/61*